Monthly Notices of the ROYAL ASTRONOMICAL SOCIETY

MNRAS **515,** L72–L77 (2022) https://doi.org/10.1093/mnrasl/slac063

Pegasus V/Andromeda XXXIV–a newly discovered ultrafaint dwarf galaxy on the outskirts of Andromeda

Michelle L. M. Collins [1]★ Emily J. E. Charles,[1] David Martínez-Delgado,[2] Matteo Monelli,[3,4] Noushin Karim,[1] Giuseppe Donatiello,[5] Erik J. Tollerud[6] and Walter Boschin [3,4,7]

[1]*Physics Department, University of Surrey, Guildford GU2 7XH, UK*
[2]*Instituto de Astrofísica de Andalucía, CSIC, Glorieta de la Astronomía, E-18080 Granada, Spain*
[3]*Instituto de Astrofísica de Canarias (IAC), Calle Vía Láctea s/n, E-38205 La Laguna, Tenerife, Spain*
[4]*Facultad de Física, Universidad de La Laguna, Avda. Astrofísico Fco. Sánchez s/n, E-38200 La Laguna, Tenerife, Spain*
[5]*UAI – Unione Astrofili Italiani /P.I. Sezione Nazionale di Ricerca Profondo Cielo, I-72024 Oria, Italy*
[6]*Space Telescope Science Institute, 3700 San Martin Drive, Baltimore, MD 21218, USA*
[7]*Fundación G. Galilei – INAF (Telescopio Nazionale Galileo), Rambla J. A. Fernández Pérez 7, E-38712 Breña Baja (La Palma), Spain*

Accepted 2022 June 2. Received 2022 May 30; in original form 2022 April 20

ABSTRACT

We report the discovery of an ultrafaint dwarf in the constellation of Pegasus. Pegasus V (Peg V)/Andromeda XXXIV was initially identified in the public imaging data release of the DESI Legacy Imaging Surveys and confirmed with deep imaging from *Gemini/GMOS-N*. The colour–magnitude diagram shows a sparse red giant branch (RGB) population and a strong overdensity of blue horizontal branch stars. We measure a distance to Peg V of $D = 692^{+33}_{-31}$ kpc, making it a distant satellite of Andromeda with $M_V = -6.3 \pm 0.2$ and a half-light radius of $r_{\rm half} = 89 \pm 41$ pc. It is located ∼260 kpc from Andromeda in the outskirts of its halo. The RGB is well fitted by a metal-poor isochrone with [Fe/H] = −3.2, suggesting it is very metal poor. This, combined with its blue horizontal branch, could imply that it is a reionization fossil. This is the first detection of an ultrafaint dwarf outside the deep Pan-Andromeda Archaeological Survey area, and points to a rich, faint satellite population in the outskirts of our nearest neighbour.

Key words: galaxies: dwarf – galaxies: individual.

1 INTRODUCTION

The last two decades have seen an explosion in the detection of faint dwarf galaxies in the Local Group (e.g. Willman et al. 2005a, b; Belokurov et al. 2006, 2007, 2008; McConnachie et al. 2008; Martin et al. 2009; Bechtol et al. 2015; Koposov et al. 2015; Torrealba et al. 2016, 2018, 2019; Mau et al. 2020; Cerny et al. 2021a, b). Wide-field imaging surveys such as the Sloan Digital Sky Survey (Abazajian et al. 2009), Pan-STARRS (Chambers et al. 2016), the Pan-Andromeda Archaeological Survey (PAndAS; McConnachie et al. 2009), the Dark Energy Survey (DES; Abbott et al. 2018), and the DECam Local Volume Exploration Survey (DELVE; Drlica-Wagner et al. 2021) have uncovered a wealth of substructures orbiting the Milky Way (MW) and Andromeda (M31) galaxies. Despite the discovery of dozens of new dwarf satellites, it is complex to reconcile their numbers with theoretical predictions (e.g. Tollerud et al. 2008; Koposov et al. 2009; Walsh, Willman & Jerjen 2009; Bovill & Ricotti 2011b; Bullock & Boylan-Kolchin 2017; Kim, Peter & Hargis 2018).

At the bright end ($L \gtrsim 10^5$ L$_\odot$), predictions and observations are in good agreement (e.g. Sawala et al. 2016; Kim et al. 2018; Read & Erkal 2019; Engler et al. 2021). As such, it is likely that the remaining gap will be resolved as we push to ever-lower luminosities with new surveys, such as the Vera C. Rubin Legacy Survey of Space and Time (Tollerud et al. 2008; Bovill & Ricotti 2011a). In M31, detection of the faintest galaxies has been limited to the central 150 kpc probed by PAndAS, which has discovered dwarf galaxies down to $L \sim 2 \times 10^4$ L$_\odot$ ($M_V \sim -6$; e.g. McConnachie et al. 2009; Richardson et al. 2011; Martin et al. 2013b). Work by Martin et al. (2016) demonstrated that there are likely many more faint dwarfs lurking just below the detection limit of the survey, and discoveries of brighter dwarfs at much greater distances ($\gtrsim$ 200 kpc) in shallower surveys (Martin et al. 2013a, c) suggest that there is a wealth of galaxies to be found out to the virial radius of the system.

These faintest dwarfs provide tight constraints on reionization and stellar feedback physics as their gas reservoirs can more easily escape their low-mass potentials. Deep imaging studies with the *Hubble Space Telescope* have shown that ultrafaint dwarfs (UFDs) tend to have their star formation quenched early (e.g. Brown et al. 2014; Sacchi et al. 2021), representing the relics of the very first galaxies (Bovill & Ricotti 2009). They are also extremely dark matter dominated (e.g. Martin et al. 2007; Simon & Geha 2007; Geha et al. 2009; Simon 2019) and so their detection and further study may allow us insight into the nature of the dark matter particle.

With the value of finding new dwarfs to address these problems in mind, we have been conducting a visual inspection of imaging data from the DESI Legacy Imaging Survey (Dey et al. 2019) in the vicinity of M31 and Triangulum (M33) to search for ultrafaint companions to both systems. We have already identified a potential UFD satellite of M33 – Pisces VII/Triangulum III (Martínez-Delgado et al. 2022). In this paper, we report on a newly discovered UFD

★ E-mail: m.collins@surrey.ac.uk

satellite of M31 in the constellation of Pegasus – Pegasus (Peg) V/Andromeda (And) XXXIV. In Section 2, we discuss the DESI Legacy Survey imaging and our deep follow-up observations with *Gemini/GMOS-N*, then in Section 3 we present the properties of, and distance to, Peg V. Finally, we discuss the significance of our findings in Section 4.

2 IDENTIFICATION AND GEMINI OBSERVATIONS

Peg V was identified as a partially resolved overdensity in the DESI Legacy Imaging Survey (see left-hand panel of Fig. 1) by amateur astronomer Giuseppe Donatiello. Given its position on-sky, it was a good candidate for an ultrafaint M31 satellite (projected distance of ∼240 kpc). We were awarded directors discretionary time (proposal ID GN-2021B-DD-106) to perform deep imaging with *Gemini/GMOS-N* to resolve its stellar populations. Our observations were carried out on the nights of 2021 November 1 and 2021 November 25 and employed the *g*- and *r*-band filters. The total imaging time was 2250 s in *g* band (split into 5 × 450 s exposures) and 1500 s in *r* band (split into 5 × 300 s exposures). The images were pre-processed using the *Gemini* DRAGONS pipeline, which performs standard bias, flat-field, and cosmic ray corrections to the images before producing a final stacked image (which can be seen in the right-hand panel of Fig. 1). The stacked images were then reduced using DAOPHOT/ALLFRAME (Stetson 1987, 1994) in largely the same manner as Monelli et al. (2010) and Martínez-Delgado et al. (2022). Briefly, we search for stellar sources on each stacked image and then perform aperture photometry, point spred function (PSF) derivation, and PSF photometry with ALLSTAR. The resulting list of stars is then passed to ALLFRAME to construct individual catalogues with better determined position and instrumental magnitude of the input sources that provides the final photometry. We perform the photometric calibration using local standard stars from the Pan-STARRS1 3π survey (Chambers et al. 2016). The mean magnitudes were calibrated with a linear relation for the *g* band, and a zero-point for the *r* band. We extinction correct the data using the reddening maps from Schlegel, Finkbeiner & Davis (1998), recalibrated by Schlafly & Finkbeiner (2011).

Star–galaxy separation was performed using the sharpness parameter. In the left-hand panel of Fig. 2, we show the distribution of stars across the *GMOS* field of view, with the right-hand panel showing the galaxy distribution. There is a clear overdensity in the centre of the stellar map. In in the left-hand panel of Fig. 3, we show a colour–magnitude diagram (CMD) for all stars within 0.8 arcmin of this overdensity compared to an equal area annulus beyond 1.6 arcmin in the centre panel. An old (12.5 Gyr), metal-poor ([Fe/H] = −3.2) BaSTI isochrone (Hidalgo et al. 2018)[1] is overlaid, shifted to a distance of ∼700 kpc to highlight the red-giant branch (RGB) and horizontal branch (HB) feature.

3 PROPERTIES OF PEGASUS V

We determine the structural parameters for Peg V using the same Markov chain Monte Carlo (MCMC) inference technique as presented in Martínez-Delgado et al. (2022). We defer to that work for a detailed discussion, and briefly outline this process below. The method is based on that of Martin et al. (2016) and uses EMCEE (Foreman-Mackey et al. 2013) to sample the posterior. We include all stars which fall within a broad colour–magnitude cut of $r_0 < 25.5$ and $-0.5 < (g-r)_0 < 0.9$, giving 79 stars total. We then assume these stars comprise both members of the dwarf galaxy, and a foreground/background population. We assume the radial density profile, $\rho_{\rm dwarf}$ of the dwarf can be modelled as an exponential profile, with an ellipticity of $\epsilon = 1 - (b/a)$ and $r_{\rm half}$ is the half-light radius. N^* is the number of likely member stars inside the CMD selection box associated to the dwarf.

We assume the foreground/background contamination, $\Sigma_{\rm b}$, is constant across the field and determine this by subtracting the dwarf galaxy stars (which we calculate by integrating the radial density profile) from the total number of potential members identified. We combine these assumptions into a likelihood function, which is then used in the MCMC analysis:

$$\rho_{\rm model}(r) = \rho_{\rm dwarf}(r) + \Sigma_{\rm b}. \quad (1)$$

We use broad, flat uniform priors for all parameters. The EMCEE routine used 100 walkers, over a total of 10 000 iterations with a burn in of 9250. These numbers were determined based on a visual inspection of the traces. We show the results in Fig. 4 and summarize them in Table 1. We find a position for Peg V of $\alpha = 23{:}18{:}27.8 \pm 0.1$, $\delta = 33{:}21{:}32 \pm 3$, a half-light radius of $r_{\rm half} = 0.44^{+0.2}_{-0.1}$ arcmin, and do not resolve an ellipticity.

The CMD for Peg V presents us with a sparse RGB and a well-populated HB feature. Given its projected distance from Andromeda of $D_{\rm proj} \sim 245$ kpc, the most likely scenario is that Peg V is an M31 satellite. To determine its distance, we use two techniques that focus on the RGB and HB populations. For the RGB, we employ the same Bayesian tip of the red giant branch (TRGB) approach as in Tollerud et al. (2016) and Martínez-Delgado et al. (2022), which we briefly summarize below. We model the RGB and background population simultaneously as a broken power law with slopes of α and β in luminosity, respectively. We assume a fraction f of stars in the background population (such that the fraction on the RGB is $1 - f$) with the break located at the TRGB, $m_{\rm TRGB}$.

We use Bayesian inference to determine posterior probabilities for $m_{\rm TRGB}$, using uniform priors for all parameters, with U(0, 1) for f and U(0, 2) for α and β. For $m_{\rm TRGB}$, we use a broad prior of U(17, 22.5). We use the same colour selection as for the structural parameters of $(-0.5 < g - r < 0.9)$, but only include stars with $r_0 < 24$ to isolate the RGB. We use only stars within $2r_{\rm half}$, as if we include stars beyond this, the model has trouble distinguishing between background and dwarf (given the sparsity of RGB stars). We numerically integrate this luminosity function over a grid of m using the trapezoid rule for each set of parameters, and take the total likelihood as the sum of the logarithm of this over all stars.

We use EMCEE to sample the posterior distribution for the model parameters and find a solution of $m_{\rm TRGB} = 21.2^{+1.0}_{-1.8}$, corresponding to a distance of $D = 682^{+391}_{-355}$ kpc. This fit is poorly constrained owing to the small number of sources on the RGB.

A more precise distance can be determined by assuming the stars at $g_0 \sim 24.5$ constitute the HB. In the right-hand panels of Fig. 3, we show the luminosity function in the *g* band for Peg V. There is a pronounced bump at $g_0 \sim 24.8 \pm 0.1$ that we assume is the HB. With $M_{g,\rm HB} = 0.6$ (Irwin et al. 2007), we measure a distance of $D = 692^{+33}_{-31}$ kpc, entirely consistent with the RGB approach but with far smaller uncertainties.

In panel 1 of Fig. 3, we show our isochrones shifted to this distance. We see that the HB and RGB features for the 12.5 Gyr isochrone perfectly overlap with the stellar populations of Peg V, suggesting that our candidate is an extremely metal-poor M31 satellite.

[1] http://basti-iac.oa-abruzzo.inaf.it/isocs.html

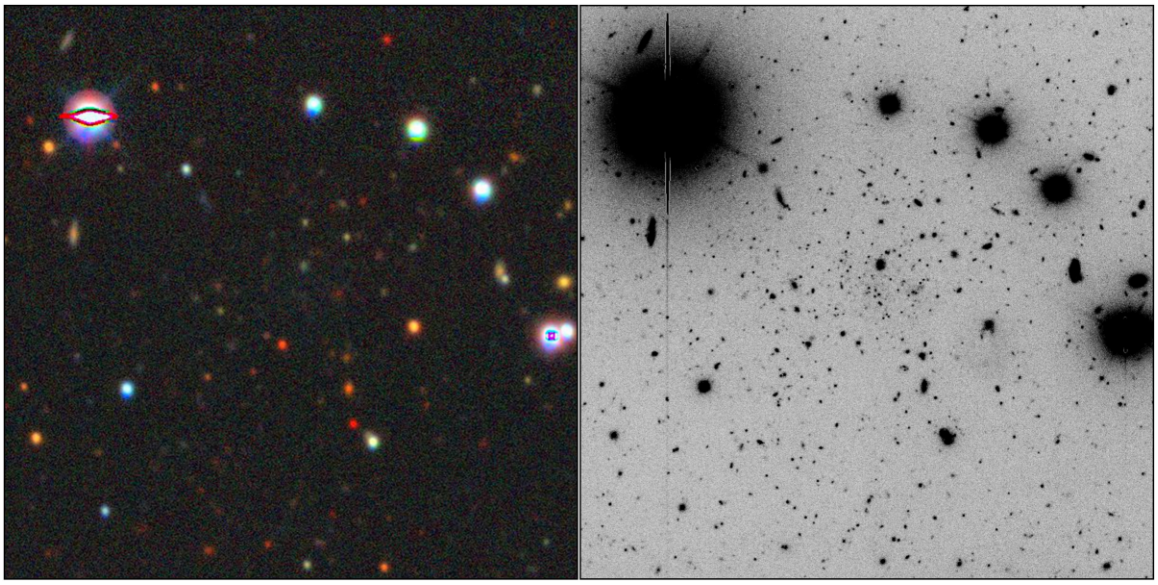

Figure 1. Left-hand panel: Image of the dwarf galaxy Peg V from the DESI Legacy Imaging Survey. Right-hand panel: *Gemini/GMOS-N* combined *g*- and *r*-band image of the galaxy obtained from *Gemini* follow-up observations (see Section 2). North is up, east is left. In both images, the field of view is 150 arcsec × 150 arcsec.

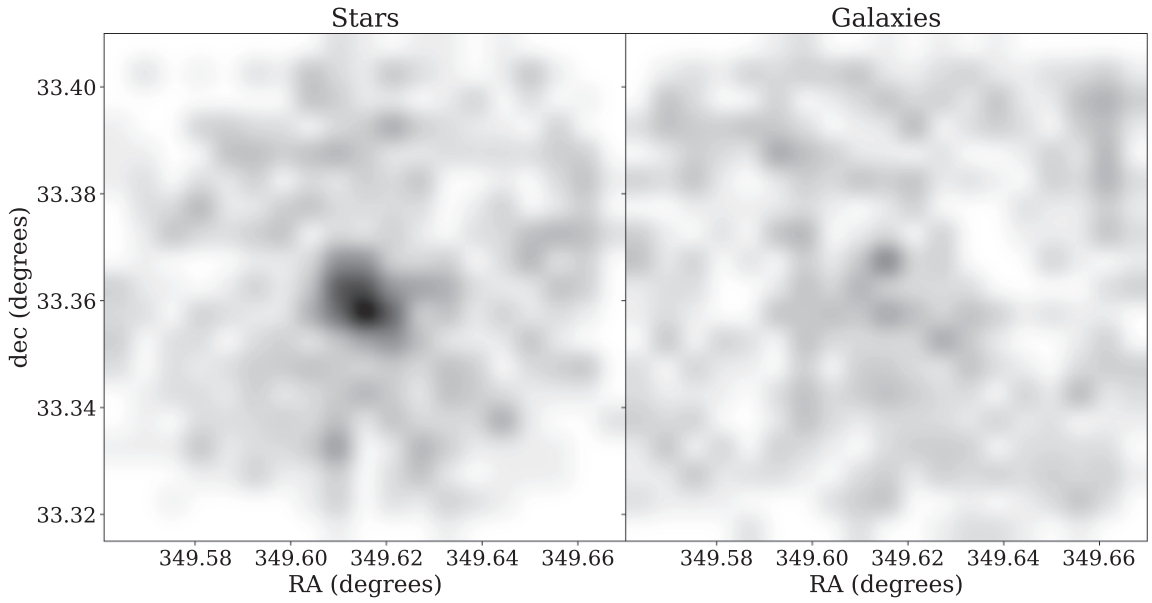

Figure 2. Filtered maps of all sources considered stars (left) versus galaxies (right) within our *GMOS-N* field of view. A clear overdensity is seen in the stellar map that is not reproduced in the galaxies panel.

Armed with a distance, we follow the approach of Martin et al. (2016) and Martínez-Delgado et al. (2022) to measure the luminosity of Peg V. Using theoretical luminosity functions generating the PARSEC stellar models (Marigo et al. 2008; Girardi et al. 2010), we define a probability distribution function (PDF), which describes the expected number of RGB stars per magnitude bin. We use an old (12 Gyr), metal-poor ([Fe/H] $= -2.5$), and α enhanced ([α/Fe] $= +0.4$) isochrone with a Kroupa initial mass function. We randomly sample from this luminosity function to reproduce our observed dwarf, which is simplified as having N^* stars (where N^* is taken from our MCMC analysis) above our magnitude cut of $r_0 < 25.5$. We record the sampled magnitude for all stars above and below this cut. Once N_* is reached, we sum all stars that were randomly sampled to get the total luminosity of Peg V. We repeat this procedure 1000 times to measure the average luminosity and a statistical uncertainty for each observed magnitude band. We then convert these to the V band to obtain $M_V = -6.3 \pm 0.2$ for a distance of $D = 692^{+33}_{-31}$ kpc where both distance and luminosity uncertainties are included.

4 DISCUSSION AND CONCLUSIONS

We have discovered a new Local Group UFD in the constellation of Pegasus and characterized it using deep *Gemini/GMOS-N* imaging. Peg V/And XXXIV is a far-flung M31 satellite with $M_V = -6.3 \pm 0.2$, located 242 kpc from the centre of the system. This

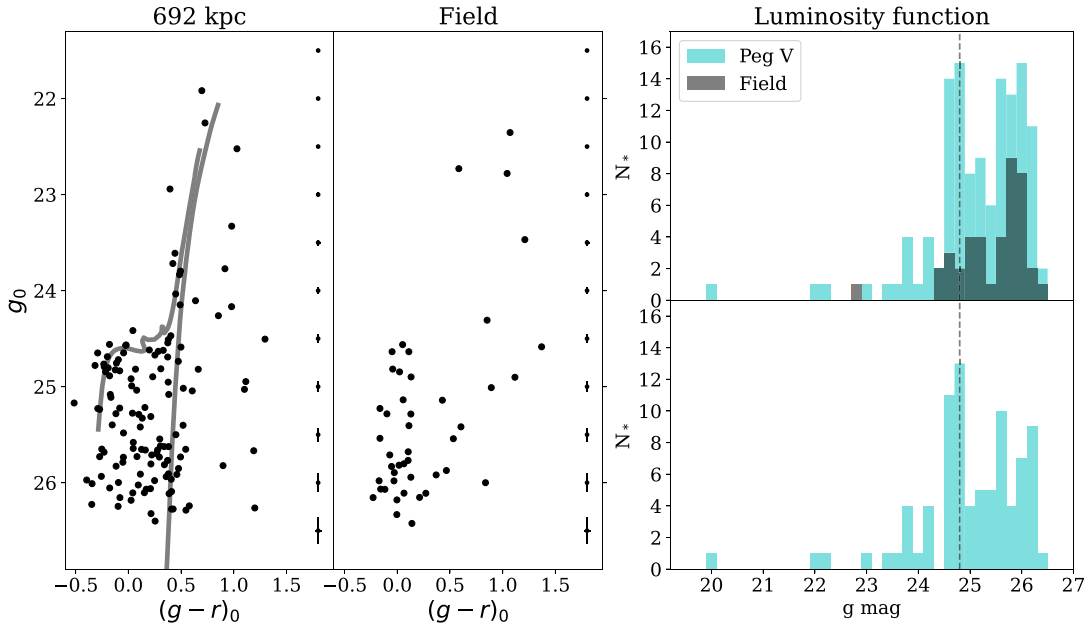

Figure 3. In the first two panels, we show the CMD for all stars within $2r_{\rm half}$ of Peg V (left) compared with the stellar populations in an equal area annulus beyond the dwarf to demonstrate the field contamination (right). We overlay a metal-poor ([Fe/H] $= -3.2$) isochrone with age 12.5 Gyr shifted to 692 kpc (centre), representing the distance measured from the HB. Finally, we show the luminosity function in the rightmost panels. The top shows all stars within $2r_{\rm half}$ (cyan) and the field population (grey), and the lower panel shows the background-corrected case. The dashed grey line shows the position of the blue HB feature.

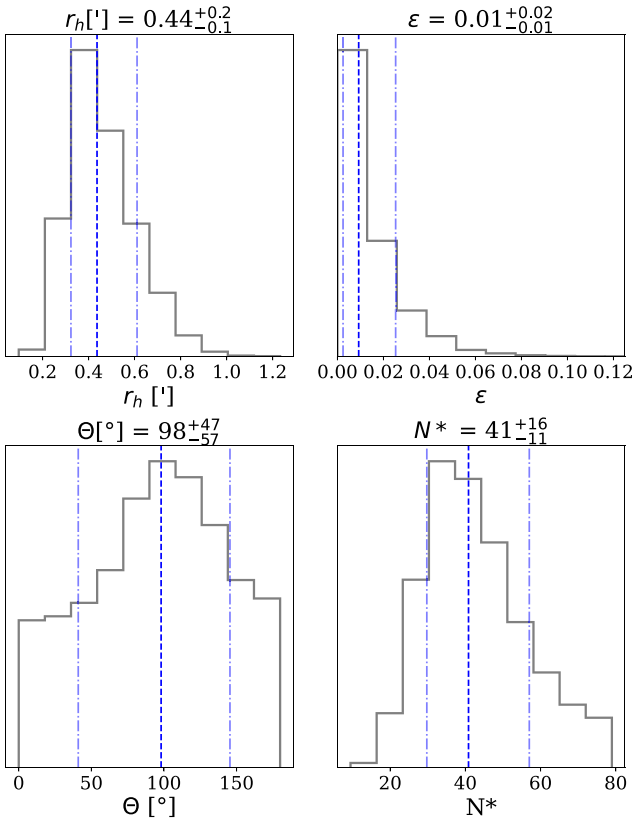

Figure 4. Marginalized posteriors for the structural parameters of Peg V. We show the the half-light radius, $r_{\rm half}$, ellipticity, ϵ, position angle, θ, and the number of stars belonging to Peg V, N^*. The dashed lines represent the median value and 1σ uncertainties.

Table 1. The final structural and photometric properties for Peg V.

Property	Value
RA	$23^{\rm h}\,18^{\rm m}\,27.8^{\rm s} \pm 0.1^{\rm s}$
Dec.	$33^\circ\,21'\,32'' \pm 3''$
$r_{\rm half}$ (arcmin)	$0.4^{+0.2}_{-0.1}$
D (kpc)	692^{+33}_{-31}
$D_{\rm M31}$ (kpc)	242^{+12}_{-11}
$r_{\rm half}$ (pc)	87^{+40}_{-54}
M_V	-6.3 ± 0.2
μ_0 (mag arcsec^{-2})	26.3 ± 0.3
L ($L_\odot$)	$2.8^{+0.6}_{-0.4} \times 10^4$
ϵ	0.01 ± 0.01
θ ($^\circ$)	96^{+47}_{-57}
N*	41^{+16}_{-11}
$E(B-V)$ (mag)	0.06

places it close to the virial radius of M31 (estimated to be between ∼250–300 kpc; e.g. Blaña Díaz et al. 2018; Kafle et al. 2018; Patel et al. 2018). It is also the faintest M31 satellite detected outside of the PAndAS Survey. Given its size and luminosity, it is most likely a dwarf galaxy. However, at the lower 1σ bound on the radius, it could be consistent with the extended globular cluster population in M31's halo (e.g. Mackey et al. 2013).

The strong blue HB of Peg V makes it somewhat unique in Andromeda. M31 dwarf satellites typically possess far redder HBs (e.g. Da Costa et al. 1996, 2000; Da Costa, Armandroff & Caldwell 2002) with only a handful showing a significant blue component. Martin et al. (2017) present homogeneous single orbit *HST* observations for 20 M31 satellite galaxies that well-resolve their HBs. They assess the colour of their HB features by computing the ratio, η, of the number

of blue HB stars ($n_{\rm BHB}$) to the total number of HB stars ($n_{\rm BHB} + n_{\rm RHB}$). They find only two examples of dwarfs with relatively high fractions of blue HB stars, giving $\eta \sim 0.4$ (And XI and XVII). Repeating their analysis for Peg V, we find $\eta = 0.5 \pm 0.2$, setting it apart from the rest of the system. As blue HB stars are typically considered to trace ancient stellar populations, this could imply Peg V was quenched very early, making it a good candidate for a reionization fossil (Bovill & Ricotti 2009). It is also more similar to the UFDs of the MW, all of which appear to have been quenched $\gtrsim$10 Gyr ago (Brown et al. 2014; Weisz et al. 2014; Sacchi et al. 2021) and possess blue HB features. The RGB stars of Peg V are also extremely blue, and are well described by the most metal-poor BaSTI isochrone (see Fig. 3). This further supports that it was rapidly quenched by reionization. If true, further study of its chemical properties may allow us to place constraints on the earliest epochs of star formation.

The RGB of Peg V also looks sparser than one may expect given its strong HB population. This may be partially explained by field contamination. Additionally, when comparing the CMD of Peg V to those of similarly bright dSphs in the MW, its RGB seems underdense, which may mean we have overestimated its luminosity. Our method is susceptible to shot-noise given the sensitivity to a few individual bright stars. However, its CMD is similar to that of And XX ($M_V = -6.4$; Martin et al. 2016). It may be that space-based imaging can allow more sophisticated modelling of the luminosity function and a robust determination of Peg V's intrinsic brightness.

With deep space-based imaging, we could further probe the star formation history of Peg V, and learn if it is a candidate for a fossil galaxy quenched by reionization. It also has a few bright RGB stars, which can be targeted with 8–10 m telescopes to measure their velocities and chemistry. Given its remote position in the halo, kinematics may also allow constraints of its orbit around M31 and the likelihood of previous interactions with its host that may also have quenched its star formation.

The discovery of Peg V in the DESI Legacy Imaging Survey bodes well for future discoveries of UFDs in M31 and the wider Local Group with current and future surveys. It paints a rosy picture for simultaneously solving both the missing satellite and field galaxy problems in our cosmic backyard. Our systematic visual inspection of the DESI images successfully detects partially resolved UFD satellites in the M31/M33 system, which might be overlooked in the automatic detection of overdensities in stellar density maps (e.g. DELVE). Thus, both approaches are extremely complementary.

ACKNOWLEDGEMENTS

DMD acknowledges financial support from the Talentia Senior Program (through the incentive ASE-136) from Secretaría General de Universidades, Investigación y Tecnología, de la Junta de Andalucía. DMD acknowledges funding from the State Agency for Research of the Spanish MCIU through the 'Center of Excellence Severo Ochoa' award to the Instituto de Astrofísica de Andalucía (SEV-2017-0709) and project (PDI2020-114581GB-C21/AEI/10.13039/501100011033).

This study is based on observations obtained at the international *Gemini Observatory*, a programme of NSF's NOIRLab, which is managed by the Association of Universities for Research in Astronomy (AURA) under a cooperative agreement with the National Science Foundation. On behalf of the *Gemini Observatory* partnership: the National Science Foundation (United States), National Research Council (Canada), Agencia Nacional de Investigación y Desarrollo (Chile), Ministerio de Ciencia, Tecnología e Innovación (Argentina), Ministério da Ciência, Tecnologia, Inovações e Comunicações (Brazil), and Korea Astronomy and Space Science Institute (Republic of Korea).

Data processed using DRAGONS (Data Reduction for Astronomy from *Gemini Observatory North and South*).

This work was enabled by observations made from the Gemini North telescope, located within the Maunakea Science Reserve and adjacent to the summit of Maunakea. We are grateful for the privilege of observing the Universe from a place that is unique in both its astronomical quality and its cultural significance.

This project used public archival data from the DESI Legacy Imaging Surveys (DESI LIS). The Legacy Surveys consist of three individual and complementary projects: the Dark Energy Camera Legacy Survey (DECaLS; Proposal ID #2014B-0404; PIs: David Schlegel and Arjun Dey), the Beijing-Arizona Sky Survey (BASS; NOAO Proposal. ID #2015A-0801; PIs: Zhou Xu and Xiaohui Fan), and the Mayall z-band Legacy Survey (MzLS; Proposal. ID #2016A-0453; PI: Arjun Dey). DECaLS, BASS, and MzLS together include data obtained, respectively, at the Blanco telescope, Cerro Tololo Inter-American Observatory, NSF's NOIRLab; the Bok telescope, Steward Observatory, University of Arizona; and the Mayall telescope, Kitt Peak National Observatory, NOIRLab. The Legacy Surveys project is honoured to be permitted to conduct astronomical research on Iolkam Du'ag (Kitt Peak), a mountain with particular significance to the Tohono O'odham Nation.

NOIRLab is operated by the Association of Universities for Research in Astronomy (AURA) under a cooperative agreement with the National Science Foundation.

This project used data obtained with the Dark Energy Camera (DECam), which was constructed by the Dark Energy Survey (DES) collaboration. Funding for the DES Projects has been provided by the U.S. Department of Energy, the U.S. National Science Foundation, the Ministry of Science and Education of Spain, the Science and Technology Facilities Council of the United Kingdom, the Higher Education Funding Council for England, the National Center for Supercomputing Applications at the University of Illinois at Urbana-Champaign, the Kavli Institute of Cosmological Physics at the University of Chicago, Center for Cosmology and Astro-Particle Physics at the Ohio State University, the Mitchell Institute for Fundamental Physics and Astronomy at Texas A&M University, Financiadora de Estudos e Projetos, Fundacao Carlos Chagas Filho de Amparo, Financiadora de Estudos e Projetos, Fundacao Carlos Chagas Filho de Amparo a Pesquisa do Estado do Rio de Janeiro, Conselho Nacional de Desenvolvimento Cientifico e Tecnologico and the Ministerio da Ciencia, Tecnologia e Inovacao, the Deutsche Forschungsgemeinschaft, and the Collaborating Institutions in the Dark Energy Survey. The Collaborating Institutions are Argonne National Laboratory, the University of California at Santa Cruz, the University of Cambridge, Centro de Investigaciones Energeticas, Medioambientales y Tecnologicas-Madrid, the University of Chicago, University College London, the DES-Brazil Consortium, the University of Edinburgh, the Eidgenossische Technische Hochschule (ETH) Zurich, Fermi National Accelerator Laboratory, the University of Illinois at Urbana-Champaign, the Institut de Ciencies de l'Espai (IEEC/CSIC), the Institut de Fisica d'Altes Energies, Lawrence Berkeley National Laboratory, the Ludwig Maximilians Universitat Munchen and the associated Excellence Cluster Universe, the University of Michigan, NSF's NOIRLab, the University of Nottingham, the Ohio State University, the University of Pennsylvania, the University of Portsmouth, SLAC National Accelerator Laboratory, Stanford University, the University of Sussex, and Texas A&M University.

BASS is a key project of the Telescope Access Program (TAP), which has been funded by the National Astronomical Observatories

of China, the Chinese Academy of Sciences (the Strategic Priority Research Program 'The Emergence of Cosmological Structures' grant # XDB09000000), and the Special Fund for Astronomy from the Ministry of Finance. The BASS is also supported by the External Cooperation Program of Chinese Academy of Sciences (grant # 114A11KYSB20160057) and Chinese National Natural Science Foundation (grant # 11433005).

The Legacy Survey team makes use of data products from the Near-Earth Object Wide-field Infrared Survey Explorer (NEOWISE), which is a project of the Jet Propulsion Laboratory/California Institute of Technology. NEOWISE is funded by the National Aeronautics and Space Administration.

The Legacy Surveys imaging of the DESI footprint is supported by the Director, Office of Science, Office of High Energy Physics of the U.S. Department of Energy under contract no. DE-AC02-05CH1123, by the National Energy Research Scientific Computing Center, a DOE Office of Science User Facility under the same contract; and by the U.S. National Science Foundation, Division of Astronomical Sciences under contract no. AST-0950945 to NOAO.

DATA AVAILABILITY

The DESI Legacy Imaging data are publicly available at www.legacysurvey.org. The *Gemini/GMOS-N* images are hosted at archive.gemini.edu/searchform. They are associated with programme ID: GN-2021B-DD-106 and made publicly available 6 months after acquisition. Reduced photometry can be obtained from the lead author upon reasonable request.

REFERENCES

Abazajian K. N. et al., 2009, ApJS, 182, 543
Abbott T. M. C. et al., 2018, ApJS, 239, 18
Bechtol K. et al., 2015, ApJ, 807, 50
Belokurov V. et al., 2006, ApJ, 647, L111
Belokurov V. et al., 2007, ApJ, 654, 897
Belokurov V. et al., 2008, ApJ, 686, L83
Blaña Díaz M. et al., 2018, MNRAS, 481, 3210
Bovill M. S., Ricotti M., 2009, ApJ, 693, 1859
Bovill M. S., Ricotti M., 2011a, ApJ, 741, 17
Bovill M. S., Ricotti M., 2011b, ApJ, 741, 18
Brown T. M. et al., 2014, ApJ, 796, 91
Bullock J. S., Boylan-Kolchin M., 2017, ARA&A, 55, 343
Cerny W. et al., 2021a, ApJ, 910, 18
Cerny W. et al., 2021b, ApJ, 920, L44
Chambers K. C. et al., 2016, preprint (arXiv:1612.05560)
Da Costa G. S., Armandroff T. E., Caldwell N., Seitzer P., 1996, AJ, 112, 2576
Da Costa G. S., Armandroff T. E., Caldwell N., Seitzer P., 2000, AJ, 119, 705
Da Costa G. S., Armandroff T. E., Caldwell N., 2002, AJ, 124, 332
Dey A. et al., 2019, AJ, 157, 168
Drlica-Wagner A. et al., 2021, ApJS, 256, 2
Engler C. et al., 2021, MNRAS, 507, 4211
Foreman-Mackey D., Hogg D. W., Lang D., Goodman J., 2013, PASP, 125, 306
Geha M., Willman B., Simon J. D., Strigari L. E., Kirby E. N., Law D. R., Strader J., 2009, ApJ, 692, 1464
Girardi L. et al., 2010, ApJ, 724, 1030
Hidalgo S. L. et al., 2018, ApJ, 856, 125
Irwin M. J. et al., 2007, ApJ, 656, L13
Kafle P. R., Sharma S., Lewis G. F., Robotham A. S. G., Driver S. P., 2018, MNRAS, 475, 4043
Kim S. Y., Peter A. H. G., Hargis J. R., 2018, Phys. Rev. Lett., 121, 211302
Koposov S. E., Yoo J., Rix H.-W., Weinberg D. H., Macciò A. V., Escudé J. M., 2009, ApJ, 696, 2179
Koposov S. E., Belokurov V., Torrealba G., Evans N. W., 2015, ApJ, 805, 130
Mackey A. D. et al., 2013, ApJ, 770, L17
Marigo P., Girardi L., Bressan A., Groenewegen M. A. T., Silva L., Granato G. L., 2008, A&A, 482, 883
Martin N. F., Ibata R. A., Chapman S. C., Irwin M., Lewis G. F., 2007, MNRAS, 380, 281
Martin N. F. et al., 2009, ApJ, 705, 758
Martin N. F. et al., 2013a, ApJ, 772, 15
Martin N. F., Ibata R. A., McConnachie A. W., Mackey A. D., Ferguson A. M. N., Irwin M. J., Lewis G. F., Fardal M. A., 2013b, ApJ, 776, 80
Martin N. F. et al., 2013c, ApJ, 779, L10
Martin N. F. et al., 2016, ApJ, 833, 167
Martin N. F. et al., 2017, ApJ, 850, 16
Martínez-Delgado D., Karim N., Charles E. J. E., Boschin W., Monelli M., Collins M. L. M., Donatiello G., Alfaro E. J., 2022, MNRAS, 509, 16
Mau S. et al., 2020, ApJ, 890, 136
McConnachie A. W. et al., 2008, ApJ, 688, 1009
McConnachie A. W. et al., 2009, Nature, 461, 66
Monelli M. et al., 2010, ApJ, 720, 1225
Patel E., Besla G., Mandel K., Sohn S. T., 2018, ApJ, 857, 78
Read J. I., Erkal D., 2019, MNRAS, 487, 5799
Richardson J. C. et al., 2011, ApJ, 732, 76
Sacchi E. et al., 2021, ApJ, 920, L19
Sawala T. et al., 2016, MNRAS, 457, 1931
Schlafly E. F., Finkbeiner D. P., 2011, ApJ, 737, 103
Schlegel D. J., Finkbeiner D. P., Davis M., 1998, ApJ, 500, 525
Simon J. D., 2019, ARA&A, 57, 375
Simon J. D., Geha M., 2007, ApJ, 670, 313
Stetson P. B., 1987, PASP, 99, 191
Stetson P. B., 1994, PASP, 106, 250
Tollerud E. J., Bullock J. S., Strigari L. E., Willman B., 2008, ApJ, 688, 277
Tollerud E. J., Geha M. C., Grcevich J., Putman M. E., Weisz D. R., Dolphin A. E., 2016, ApJ, 827, 89
Torrealba G., Koposov S. E., Belokurov V., Irwin M., 2016, MNRAS, 459, 2370
Torrealba G. et al., 2018, MNRAS, 475, 5085
Torrealba G. et al., 2019, MNRAS, 488, 2743
Walsh S. M., Willman B., Jerjen H., 2009, AJ, 137, 450
Weisz D. R., Dolphin A. E., Skillman E. D., Holtzman J., Gilbert K. M., Dalcanton J. J., Williams B. F., 2014, ApJ, 789, 147
Willman B. et al., 2005a, AJ, 129, 2692
Willman B. et al., 2005b, ApJ, 626, L85

This paper has been typeset from a TEX/LATEX file prepared by the author.